Mechanical Input Energy Optimization of Quasi-static-toggling Electromagnetic Energy Harvester

Yu Yin[a], Guobiao Hu[b], and Junrui Liang[a]

[a]School of Information Science and Technology, ShanghaiTech University, Shanghai, China
[b]Internet of Things Thrust, Hong Kong University of Science and Technology (Guangzhou), Guangzhou, China

ABSTRACT

Quasi-static-toggling (QST) electromagnetic energy harvesters are the most successful commercialized small-scale mechanical energy harvesters for self-powered wireless electronic gadgets, such as motion-powered wireless switches. However, the working principle was not seriously investigated and theoretically analyzed until recently. Given the belated attention from academia, there is still a large gap in fully understanding the QST operation and grasping its optimal energy harvesting strategy. This paper provides a parametric analysis for optimizing the mechanical input energy of a bistable QST harvester. The input energy is calculated as the stored potential energy in the energy-buffering spring before toggling or being released. Such an amount of energy correlates with the magnetic force, the distance between two magnetic poles, and the stiffness of the energy-buffering spring. On the other hand, the most considerate design as a self-powered wireless press button must also take the human factor, i.e., comfortable fingertip force, into consideration. All these factors are taken into consideration in this paper, based on a lumped model. A multi-field coupled numeric simulation is carried out using Matlab Simscape to validate the theoretical analysis. The result shows that the optimal energy input is realized when the product of magnetic pole distance and energy-buffering spring stiffness equals the magnetic attaching force. An experimental prototype is manufactured based on this guidance. Such a new insight is valuable for making effective and full use of a QST electromagnetic energy harvester.

Keywords: Quasi-static toggling, mechanical energy harvester, electromagnetic, energy analysis

1. INTRODUCTION

To harvest energy from vibration and make the otherwise wasted energy into useful electricity was first formally discussed by Williams and Yates in 1996.[1] Vibration energy harvesting (VEH) technology has been divided into several categories, according to the transduction mechanisms, i.e., electromagnetic, piezoelectric, triboelectric, magnetostrictive, and others.[2] The mechanical vibration energy can come from different scenarios, such as aviation,[2] railway,[3] roadway,[4] etc. Electromagnetic energy harvesting (EMEH) is based on the classical principle of electromechanical induction. As one of the most widely studied energy harvesting (EH) technologies, it has the advantages of relatively high electromechanical conversion coefficients, relatively large output current, etc.[4] The classical electromagnetic induction machine is utilized to generate power under rotational motions. A large portion of recent research works also studied the rotational EMEH harvester.[5–7] Most rotational induction machines have bulky armature or permanent magnets. They are more suitable to be used in relatively large displacement applications by converting the translational motion into rotational movement. For the small displacement reciprocal vibration, translational EMEH harvesters are usually utilized. Those translational energy harvesters are divided into two categories: linear harvester[8,9] and nonlinear harvester.[10,11] Linear energy harvesters have the advantage of high response near the resonant frequency. The nonlinear EMEH harvesters are developed to broaden the response bandwidth, such that the energy harvester can catch more energy under the off-resonance frequency range.

Most studies of VEH consider the power generation issue of continuously moving objects. When the input energy is an instantaneous excitation or an extremely low-speed vibration source, the design and analysis of

Correspondence author: Junrui Liang (email: liangjr@shanghaitech.edu.cn)

Active and Passive Smart Structures and Integrated Systems XVIII, edited by Serife Tol, Guoliang Huang, Xiaopeng Li, Mostafa A. Nouh, Shima Shahab, Jinkyu Yang, Proc. of SPIE Vol. 12946, 129460W · © 2024 SPIE · 0277-786X · doi: 10.1117/12.3011236

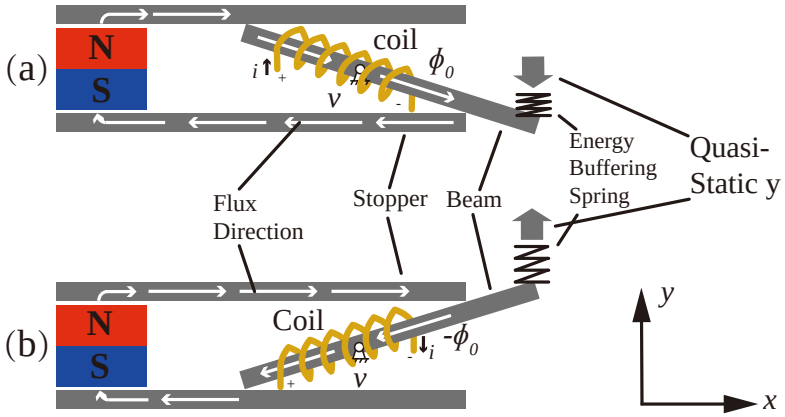

Figure 1. Working principle of QST-EMEH. (a) and (b) Two stable conditions in the bistable design.

conventional power generators are no longer suitable for these sorts of energy harvesters. To handle such a problem, one of the most promising solutions called the quasi-static-toggling (QST) energy harvester by Liu et al[12] was first commercialized by EnOcean GmbH.[13] The QST-EMEH is developed based on the instantaneous magnetic poles swapping principle.[14] The basic structure of the harvester is shown in Fig. 1. The harvester contains an iron beam as the mover. The magnetic flux flows out from a permanent magnet and is guided by two iron stoppers to flow through the mover iron beam. A coil is wounded along the iron mover based on electromagnetic induction. An energy buffering spring is also necessary to facilitate the energy conversion process. When we press or lift the free end of the energy buffering spring, energy is input into the system in the form of elastic potential energy. After the critical positions, the stored energy is rapidly converted into electrical form when the iron mover quickly swaps between the two stable positions, which is shown in Fig. 1(a) and (b). These compact energy harvesting modules were massively produced and launched into the market as commercial electronic gadgets over a decade. Yet, it was not seriously taken until a recent study from the authors' research group.[12] In this first study, the working principle and benefits of the QST mechanism for energy harvesting from very slow motion were analyzed. In particular, the significant effect of the energy buffering spring is emphasized. According to the operation in the toggling instants, the energy buffering spring was qualitatively classified into soft and hard spring cases.

In this paper, we further provide a quantitative analysis of the boundary between "soft" and "hard". A clear idea about this boundary helps further energy optimization. Section 2 explains the working principle of the QST-EMEH under the soft and hard spring cases. Section 3 provides the analysis and calculation of the input energy. Section 4 gives a simulation result to validate the theoretical analysis. Section 5 shows an experiment result. Section 6 concludes the paper.

2. WORKING PRINCIPLE

The working principle of the QST-EMEH is shown in Fig 2. $F_{g,m}$ is the magnetic adhesive force attracting the iron beam. In both the soft spring and hard spring cases, as shown in the subfigures of Fig. 2(a) and (b), points A and G are the free positions of the energy buffer spring under either of the two stable states. At these points, no force is exerted on the spring. When a compressing force is exerted on the spring, the spring deforms and accumulates elastic potential energy, as shown by point B in Fig. 2. As the compressing force increases, the system will attain the critical point C, after which the iron bar breaks the adhesion of the magnetic force. The iron beam rotates around the center axis and arrives at point D. In the soft spring case, as shown in Fig. 2(a), only part of the accumulated energy is released. The iron beam arrives at the other stable position. While in the hard spring case, almost all energy is released. The iron beam stops in the midway, as shown in Fig. 2(b). If we continue to press the spring, it continues to deform and accumulate energy. However, the beam displacement is confined by the stopper. After the position of point F, the iron beam stays at the other stable position even when the compressing force is removed.

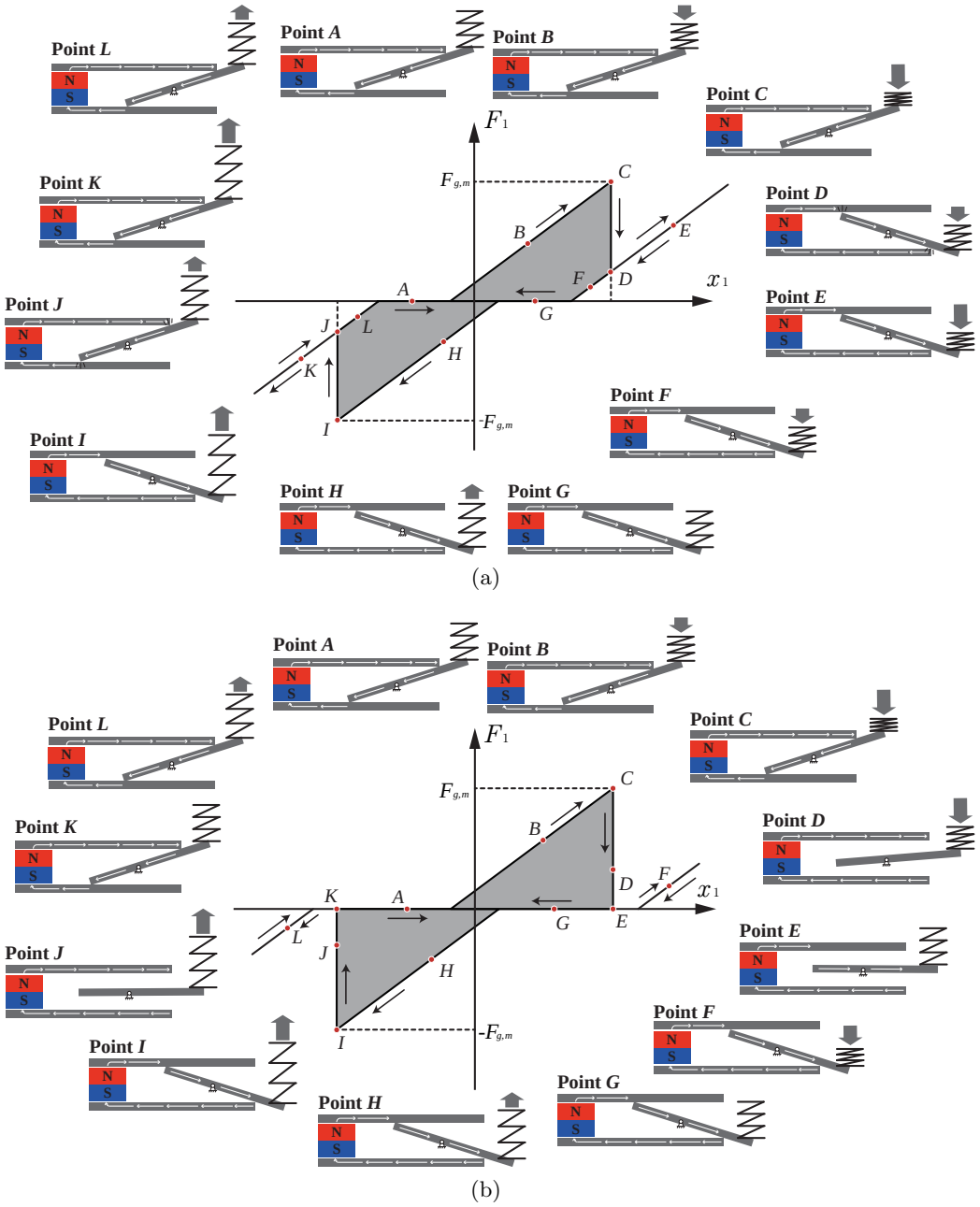

Figure 2. Working principle of QST-EMEH in (a) soft spring case, (b) hard spring case.

For the other half operating process, i.e., lifting the iron bar back to the opposite stable position from point G to point A, the working process is just symmetric. The force-displacement relation, as illustrated in the center of Fig. 2(a) and (b), shows the working paths of the QST harvester. Such an analysis of the work cycle hysteresis is usually used to show an intuitive impression of the energy removed from the system in each cycle since the enclosed area is proportional to the energy loss.[15]

A former study of the QST-EMEH[12] has qualitatively shown that the stiffness of the energy buffering spring has a significant influence over the energy harvesting performance. The boundary between soft and hard spring cases has not been clarified yet. This specific issue is extensively discussed in this paper, to offer a qualitative design guideline for the QST-EMEH design.

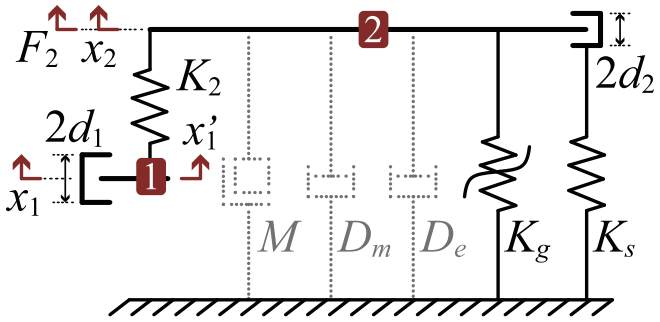

Figure 3. Mechanical lumped model of QST-EMEH.

3. MECHANICAL INPUT ENERGY

3.1 Model

The mechanical model of a bistable QST-EMEH is shown in Fig 3. Spring K_2 is the energy buffering spring. Node 1 is the place where excitation force is exerted. Node 2 represents the iron beam mover of the QST-EMEH. The beam's movement is confined within a distance of $2d_2$. The magnetic attracting force is modeled with a nonlinear stiffness K_g. The stiffness of the stoppers is also taken into consideration as K_s. The effects of the mass and damping components are neglected before toggling. Therefore, we should only consider the joint effect of K_2, K_g, and K_s during the quasi-static excitation process. The external force is passed to node 1 through another moving stopper. Such modeling is used to consider the case when the action point may go out of the finger after passing the critical position.

From the model, the force at node 2 can be expressed as follows

$$\begin{aligned} F_2(x_1, x_2) &= F_{K_2} + F_g + F_{K_s} \\ &= -K_2(x_2 - x_1') + F_g - K_s[(x_2 - d_2)H(x_2 - d_2) + (x_1 + x_2)H(-x_2 - d_2)]. \end{aligned} \tag{1}$$

In (1), F_2 is the force at node 2. x_1 is the movement of the stopper at node 1. x_1' is the movement of node 1. x_2 is the movement of the beam mover. F_{K_2} is the force applied by the energy buffering spring. F_g is the force caused by magnetic adhesion. F_{K_s} is the obstructive force of the iron stoppers. K_2 is the stiffness of the energy buffering spring. K_s is the stiffness of the iron stopper, which is usually very large. d_2 is half of the distance between two iron stoppers. $H(\cdot)$ is the Heaviside step function. The expression of x_1' is given as follows

$$x_1' = \begin{cases} x_1 - d_1, & x_2 < x_1 - d_1; \\ x_1 + d_1, & x_2 > x_1 + d_1; \\ x_2, & \text{others.} \end{cases} \tag{2}$$

The magnetic adhesive force from the two iron stopper is expressed as follows

$$F_g(x_2) = \frac{\alpha^2 \phi_0^2 d_2^3 x_2}{\mu_0 \mu_r A\left[(\alpha+1)d_2^2 - x_2^2\right]^2}. \tag{3}$$

In (3), α is a reluctance ratio. ϕ_0 is the total magnetic flux flowing through the mover iron beam. μ_0 is the vacuum permeability. μ_r is the relative magnetic permeability of the material (air in this study). A is the cross-sectional area of the magnetic circuit in square meters. When the system stays at point A, as shown in Fig 2(a). x_2 rests at the upper stopper; therefore, we have $x_2 = d_2$. Substituting this condition into (3), we got

$$F_{g,m} = \frac{\phi_0^2}{\mu_0 \mu_r A}. \tag{4}$$

In (4), the parameters μ_0 and μ_r are constant numbers. the cross-sectional area A between the stopper and moving beam interface is also regarded as a constant. Therefore, $F_{g,m}$ is proportional to the square of the magnitude flux ϕ_0. The potential energy of the magnetic assembly can be further formulated as follows

$$U_g(x_2) = \int -F_g(x_2)\mathrm{d}x_2 = -\frac{\alpha^2\phi_0^2 d_2^3}{\mu_0\mu_r A}\int \frac{x_2}{\left[(\alpha+1)\,d_2^2 - x_2^2\right]^2}\mathrm{d}x_2 = -\frac{\alpha^2\phi_0^2 d_2^3}{2\mu_0\mu_r A\left[(\alpha+1)\,d_2^2 - x_2^2\right]}. \tag{5}$$

The total potential energy of a QST-EMEH consists of the energy of the rebounding spring, the energy of the energy buffering spring, the energy of the magnetic assembly, and the energy of the stoppers. Given that x_1, the excitation position changes very slowly, the potential energy as a function of x_2 in a specific quasi-static x_1 case is expressed as follows

$$\begin{aligned} U(x_1,x_2) &= U_{k_2} + U_g + U_{k_s} = \int -F_2(x_1,x_2)\,\mathrm{d}x_2 \\ &= \frac{1}{2}K_2(x_2 - x_1')^2 - \frac{\alpha^2\phi_0^2 d_2^3}{2\mu_0\mu_r A\left[(\alpha+1)\,d_2^2 - x_2^2\right]} \\ &\quad + \frac{1}{2}K_s[(x_2-d_2)^2\,H\,(x_2-d_2) + (x_2+d_2)^2\,H\,(-x_2-d_2)]. \end{aligned} \tag{6}$$

3.2 Soft Spring Case

Given the potential energy expressed in (6), at the critical toggling point C in Fig. 2(a), the iron beam mover is going to leave the stopper. The stopper force F_{K_s} is zero. The sum of forces F_2 is also zero at the equilibrium condition. Therefore, we have

$$F_2(x_1,x_2) = -K_2(x_2 - x_1') + F_{g,m} = 0. \tag{7}$$

Rearranging (7), we have

$$x_1' = d_2 - \frac{F_{g,m}}{K_2}. \tag{8}$$

Substituting (8) into (6), we have

$$U(x_1,x_2) = \frac{1}{2}K_2\left(x_2 - d_2 + \frac{F_{g,m}}{K_2}\right)^2 - \frac{\alpha^2\phi_0^2 d_2^3}{2\mu_0\mu_r A[(\alpha+1)d_2^2 - x_2^2]}. \tag{9}$$

The input energy of once pressing down action is expressed as follows

$$E_{in} = U(x_1,d_2) - U(x_1,-d_2) = 2d_2\left(F_{g,m} - K_2 d_2\right). \tag{10}$$

The force-displacement cycle in operation with the soft spring case is illustrated in Fig. 2(a).

3.3 Hard Spring Case

For the hard spring case, after the toggling moment, the iron mover cannot immediately arrive at the opposite stopper, because of the stiff buffer spring. It is much easier to calculate the input energy according to the force-displacement diagram. From Fig. 2(b), the input energy is proportional to the area enclosed by the triangle in the first quadrant, which is formulated as follows

$$E_{in} = \frac{F_{g,m}^2}{2K_2}. \tag{11}$$

The boundary between the soft and hard spring cases can be observed when the iron mover just attains the opposite stopper with zero force F_1. The relation under the boundary condition can be formulated as follows

$$2d_2K_2 = F_{g,m}. \tag{12}$$

Table 1. Parameters for studying the input mechanical energy.

Parameter	Value/Range	Description
K_2 (N/m)	$[0, 3000]$	Stiffness of energy buffer spring
A (mm^2)	15	Cross-section area
μ_0 (H/m)	$4\pi \times 10^{-7}$	Permeability of vacuum
μ_r	1	Relative permeability of air
d_2 (mm)	$[0, 35]$	Half distance between stoppers
ϕ_0 (μWb)	20	Magnetic flux through the beam & stopper interface
α	0.1	Ratio of flux leakage

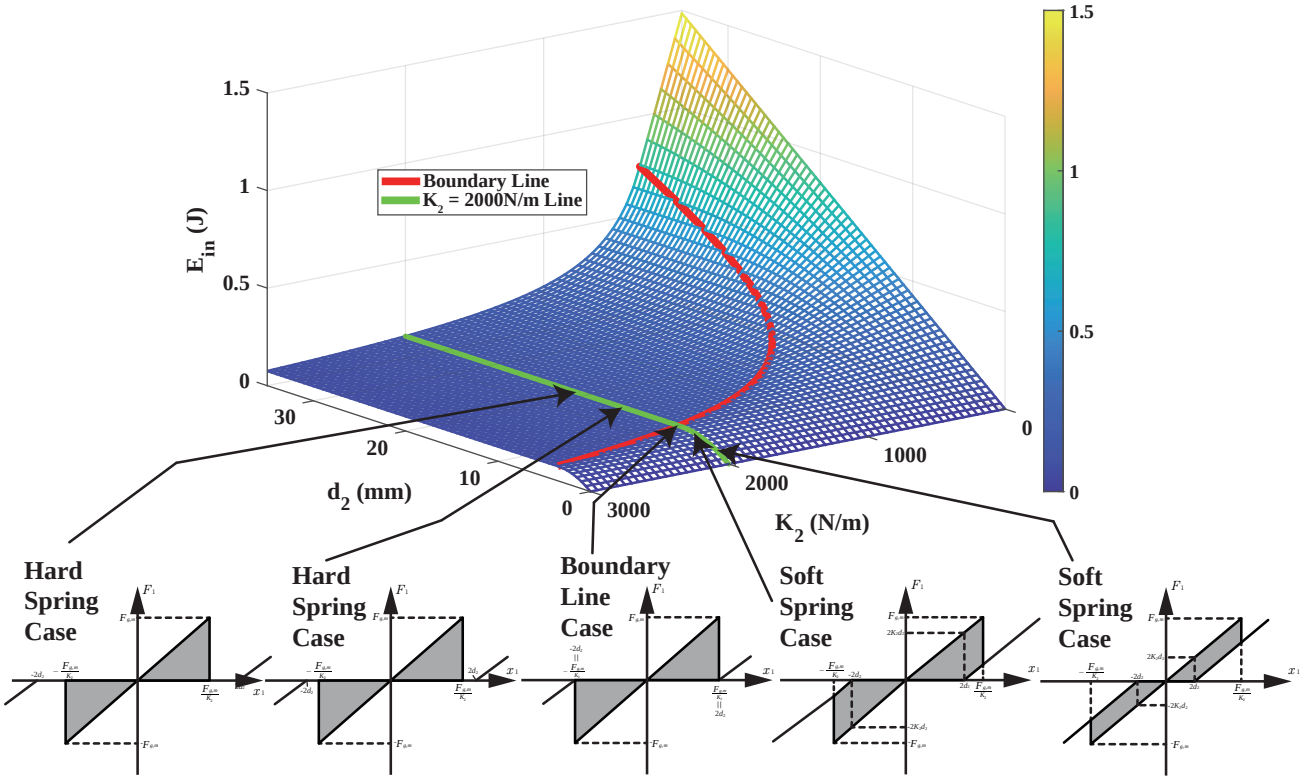

Figure 4. Input mechanical energy E_in as a function of K_2 and d_2.

Combining both soft and hard energy buffering spring cases, the mechanical input energy is formulated as follows

$$E_{in} = \begin{cases} 2d_2(F_{g,m} - K_2 d_2), & 2d_2K_2 < F_{g,m} \text{ (soft-spring case)}, \\ \frac{F_{g,m}^2}{2K_2}, & 2d_2K_2 \geq F_{g,m} \text{ (hard-spring case)}. \end{cases} \tag{13}$$

Given the parameter provided in Table 1, we formulate the input mechanical energy as a function of the buffering spring stiffness K_2 and a half of the stoppers' distance d_2. Such a functional relation is illustrated with the 3D plot shown in Fig. 4. In Fig. 4, the boundary red line cut the surface into two sections. Generally speaking, the soft-spring case gives more energy than the hard-spring case. In the soft-spring case, the input energy positively correlates with the magnetic flux ϕ_0 and also the distance between two stoppers $2d_2$. On the other hand, in the hard-spring case, the input energy only positively correlates with the flux ϕ_0. It does not change with the distance between two stoppers, i.e., $2d_2$.

4. SIMULATION

From the former analysis, we can find out that the input energy can be calculated by the distance of the stopper $2d_2$, the magnetic adhesive force $F_{g,m}$, and the stiffness of the energy-buffering spring K_2. In this section, a

Table 2. Parameters in the simulation model.

Parameters	Value/Range	Description
K_2 (N/m)	$[0, 10000]$ (default: 2000)	Energy buffer spring stiffness
D_m [μN/(m/s)]	10	Effective damping
M (g)	1	Effective mass
K_s (GN/m)	10	Stiffness of the stopper
D_s (GN/(m/s))	10	Damping coefficient of the stopper
d_2 (mm)	$[1, 30]$ (default: 3)	Half distance between stoppers
ϕ_0 (μWb)	20	Magnetic flux of beams' interface
A (mm^2)	15	Cross-section area
N (turns)	500	Turn number of the coil
R (Ω)	30	Resistance of the coil
C_r (μF)	(1,3.3,10,21,33,47,100,210,300,470,1000)	Energy storage capacitor
R_l (GΩ)	10	Load resistance
V_d (V)	0.562	Voltage drop of a diode

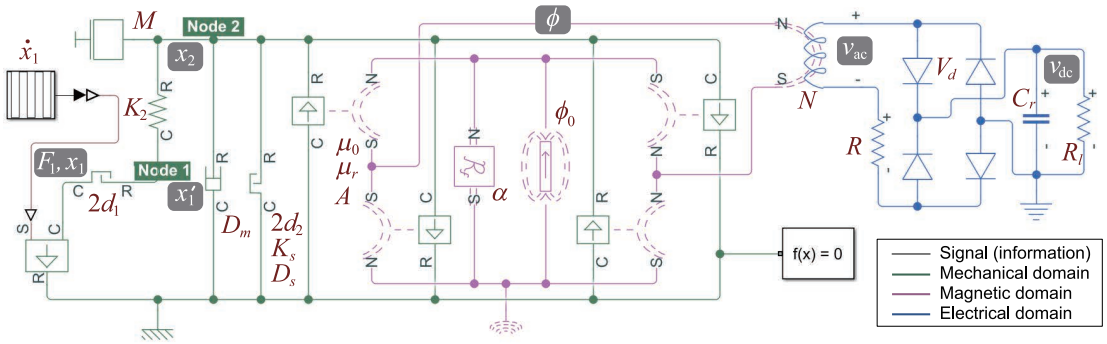

Figure 5. Dynamic model of a QST-EMEH built with Matlab Simscape.

cross-coupling dynamic model is built with Matlab Simscape, a software simulator, to validate the correctness of the formulated input energy.

4.1 Model and Parameters

The model of a QST-EMEH for simulation study is shown in Fig. 5. The black lines and blocks represent the signal domain for waveform generation, etc. The green ones represent the mechanical domain. In this study, it consists of the energy buffering spring K_2, the equivalent mass M, the equivalent mechanical damper D_m, the stopper with stiffness K_s, and the mechanical part of four transducers from the mechanical to the magnetic domain. The purple ones are in the magnetic domain. The main components of this field are the magnetic parts of four magneto-mechanical transducers and that of an induction coil, one magnetic leakage resistance, and a magnetic source ϕ_0. The blue lines represent parts in the electrical domain. The main components include the induction coil and its series resistance R, a full bridge rectifier, a filter capacitor C_r, and a load resistance R_l.

Table 2 lists the parameters used in the simulation. The table shows that K_2, d_2, and C_r are variables. Different values are selected in the simulation to generate the results under different operational conditions. Most of the parameters used in the simulation are selected the same as those in the theoretical part for better comparison between the theoretical and numerical results.

4.2 Results

The result obtained from the simulation analysis is shown in Fig. 6. The theoretically obtained results are also put in the same figures for comparison. Despite some differences in numerical values, the trend of the theoretical and simulation results is consistent. From Fig. 6(a), there is an energy difference ΔE between the simulation and theoretical results. The main reason is that, in the theoretical study, we treat the toggling process (magnetic

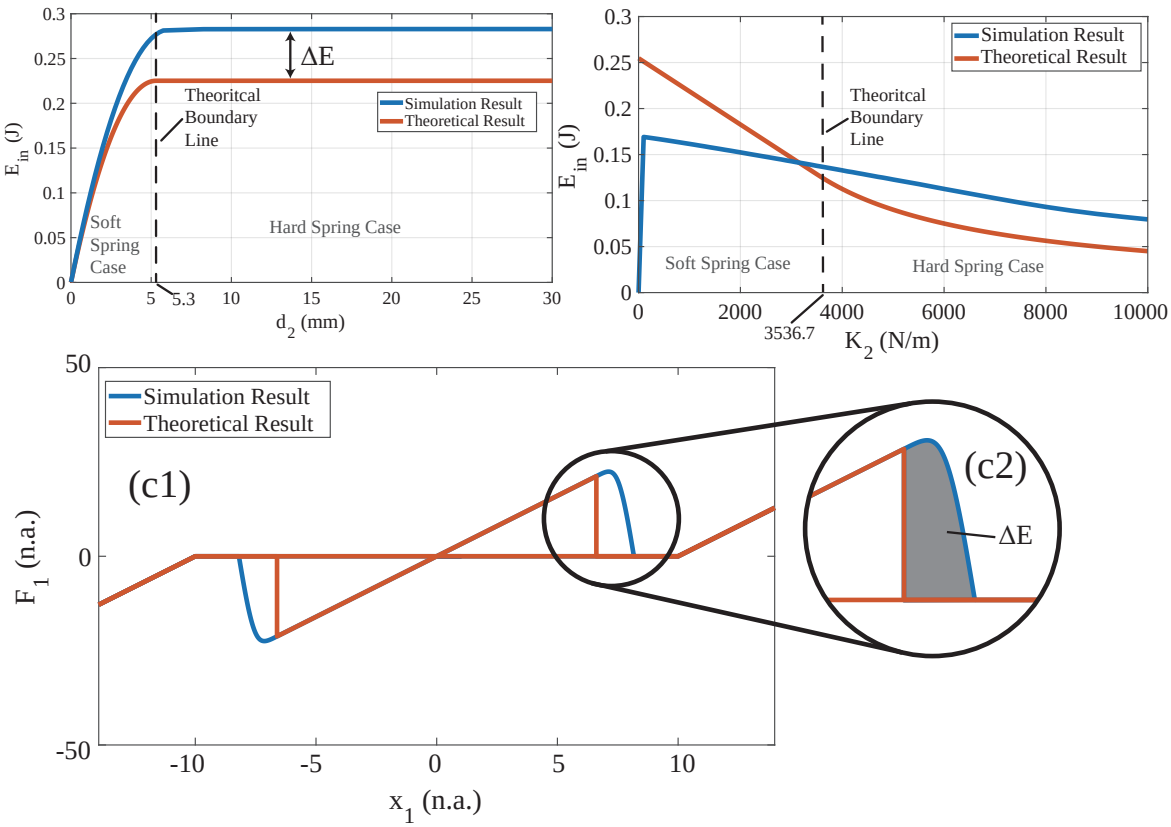

Figure 6. Simulation results of the QST-EMEH. (a) Comparison between the theoretical and simulation results under different stopper distance $2d_2$. (b) Comparison between the theoretical and simulation results under different energy buffering spring stiffness K_2. (c) An observation explaining the energy difference between theory and numerical (simulation) results.

pole swapping) as an instant event that happens in zero time. However, in the numeric simulation as well as the real dynamic system, such a toggling process takes some time to proceed. Figure 6(c) shows the difference in the force-displacement hysteresis.

Fig. 7 further gives more results about the mechanical input energy, electrical output energy, and energy conversion efficiency under different parameters, which are obtained in simulation. From Fig. 7(a) and (b), we can observe that the variation of the electrical buffering capacitance does not influence the amount of input energy. But it has a big influence on the output electrical energy. From Fig. 7(c), we can see that the trend of the output energy has a steep increase at small stoppers distance d_2. It becomes insensitive at large d_2 values. Such a phenomenon results from the cancellation of attracting magnetic force from two poles at a small distance d_2. The shorter d_2, the more cancellation effect; therefore, the lower output electrical energy. The output electrical energy peaks at a certain value of distance d_2, as we can see in Fig. 7(c). However, since the analysis involves a complicated dynamic interaction, it is not ready to be theoretically formulated. Simulation is utilized to suggest a numerical result under a specific set of parameters. More studies should be carried out in the future to better generalize the output energy expression.

5. CONCLUSION

The energy optimization of quasi-static toggling (QST) electromagnetic energy harvesters (EMEH) was only carried out by trial and error, although successful products have been already commercialized for more than a decade. This paper delivered a parametric analysis toward the mechanical input energy optimization of a QST-EMEH. The quantitative boundary between the soft and hard energy buffering springs is clarified for the first

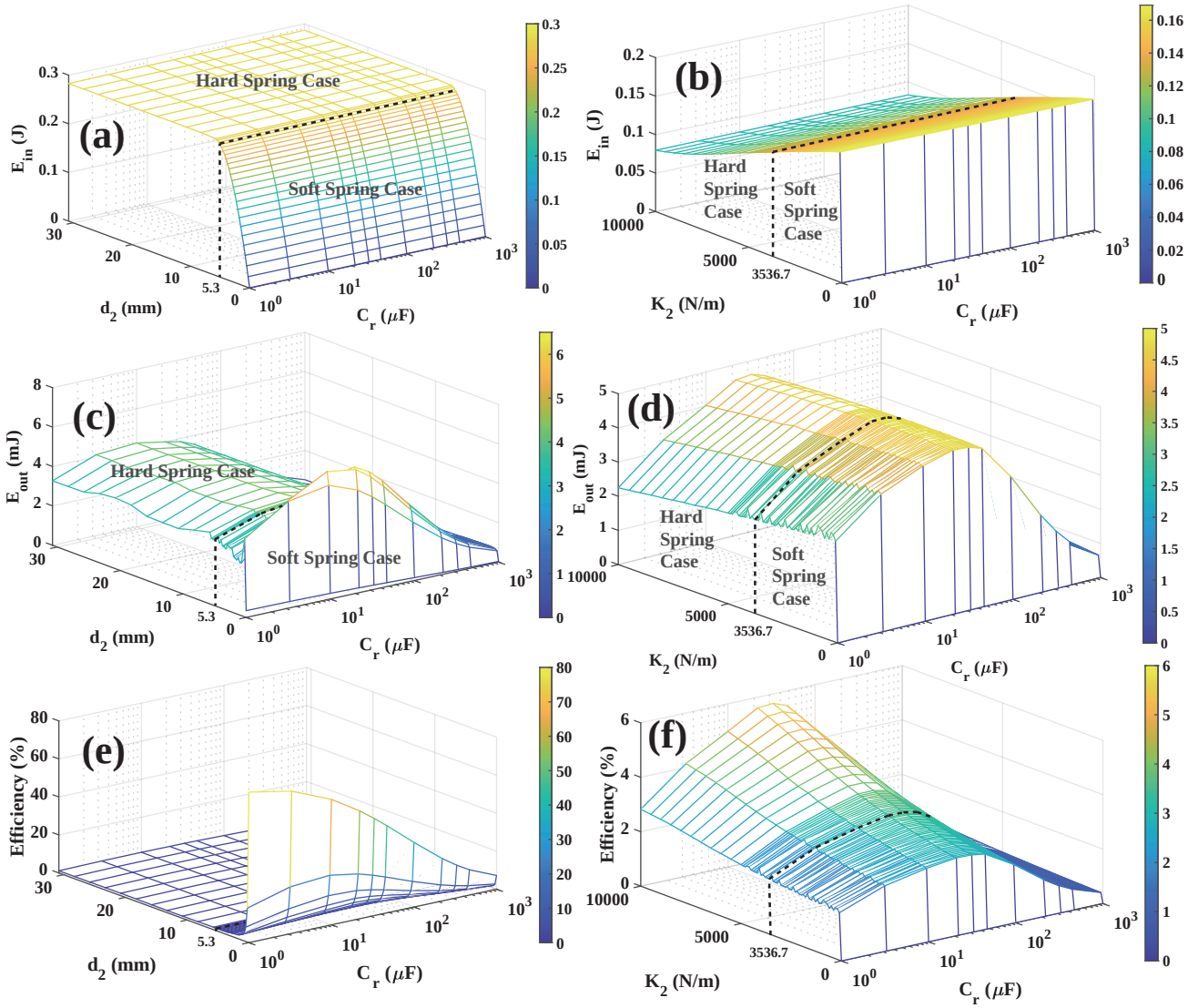

Figure 7. More results in simulation. (a) Mechanical input energy under different storage capacitance C_r and stoppers' distance $2d_2$. (b) Input mechanical energy under different storage capacitance C_r and energy buffering spring's stiffness K_2. (c) Output electrical energy under different C_r and d_2. (b) Output electrical energy under different C_r and K_2. (e) Energy conversion efficiency under different C_r and d_2. (f) EfficEnergy conversion efficiency under different C_r and K_2.

time. Generally speaking, a soft spring provides more input energy when being toggled. The output electrical energy and energy conversion efficiency were also numerically studied with a cross-coupled simulation model. More investigations should be further carried out to better understand the energy conversion detailed dynamics from the mechanical input to electrical output energy. On the other hand, although a soft spring gives more energy, it also increases the stroke distance of the finger press motions. Human comfort or user experience should be also taken as an important factor in systematic optimization as well in future work.

REFERENCES

[1] Williams, C. and Yates, R. B., "Analysis of a micro-electric generator for microsystems," *sensors and actuators A Physical* **52**(1-3), 8–11 (1996).

[2] Zelenika, S., Hadas, Z., Bader, S., Becker, T., Gljušćić, P., Hlinka, J., Janak, L., Kamenar, E., Ksica, F.,

Kyratsi, T., et al., "Energy harvesting technologies for structural health monitoring of airplane components—a review," *Sensors* **20**(22), 6685 (2020).

[3] Duarte, F. and Ferreira, A., "Energy harvesting on railway tracks: State-of-the-art," in [*Proceedings of the Institution of Civil Engineers-Transport*], **170**(3), 123–130, Thomas Telford Ltd (2017).

[4] Gholikhani, M., Roshani, H., Dessouky, S., and Papagiannakis, A., "A critical review of roadway energy harvesting technologies," *Applied Energy* **261**, 114388 (2020).

[5] Jintanawan, T., Phanomchoeng, G., Suwankawin, S., Kreepoke, P., Chetchatree, P., and U-viengchai, C., "Design of Kinetic-Energy harvesting floors," *Energies* **13**, 5419 (Oct. 2020).

[6] Liu, M., Lin, R., Zhou, S., Yu, Y., Ishida, A., McGrath, M., Kennedy, B., Hajj, M., and Zuo, L., "Design, simulation and experiment of a novel high efficiency energy harvesting paver," *Appl. Energy* **212**, 966–975 (2018).

[7] Wang, L., Todaria, P., Pandey, A., O'Connor, J., Chernow, B., and Zuo, L., "An electromagnetic speed bump energy harvester and its interactions with vehicles," *IEEE ASME Trans. Mechatron.* **21**, 1985–1994 (Aug. 2016).

[8] Cho, S. J. and Kim, J. H., "Linear electromagnetic electric generator for harvesting vibration energy at frequencies more than 50 hz," *Advances in Mechanical Engineering* **9**(10), 1687814017719001 (2017).

[9] Partodezfoli, M., Rezaey, A., Baniasad, Z., and others, "A novel speed-breaker for electrical energy generation suitable for elimination of remote parts of power systems where is near to roads," *Journal of Basic and* (2012).

[10] Sun, S., Dai, X., Wang, K., Xiang, X., Ding, G., and Zhao, X., "Nonlinear electromagnetic vibration energy harvester with closed magnetic circuit," *IEEE Magnetics Letters* **9**, 1–4 (2018).

[11] Yu, N., Fei, X., Wu, C., and Yan, B., "Modeling and analysis of magnetic spring enhanced lever-type electromagnetic energy harvesters," *Applied Mathematics and Mechanics* **43**(5), 743–760 (2022).

[12] Liu, S., Li, X., Teng, L., Hu, G., and Liang, J., "Energy and dynamic analysis of quasi-static toggling mechanical energy harvester," *Nano Energy* **104**, 107887 (2022).

[13] EnOcean, *ECO 200 Data Sheet.* (2021).

[14] Schmidt, F., *Electromagnetic energy transducer (US patent)* (2021).

[15] Liang, J. and Liao, W.-H., "Energy flow in piezoelectric energy harvesting systems," *Smart Mater. Struct.* **20**, 015005 (Dec. 2010).